CURRENT AND TRANSMISSION MEASUREMENT CHALLENGES FOR HIGH INTENSITY BEAMS

P.-A. Duperrex*, M. Gandel, D. Kiselev, Y. Lee, U. Müller, PSI, Villigen, Switzerland

Abstract

Current measurements for high intensity beams present some challenges for monitors located behind a target due to the heat load from the scattered particles. The resulting resonance drifts make accurate current and transmission measurements very difficult. These problems will become more severe with higher intensity beam operation (3mA, 1.8MW) in the PSI cyclotron. This paper presents the techniques that have been developed to overcome this problem. The present solution is based on an innovative scheme to measure on-line the resonator gain and to correct the estimate of the current.

INTRODUCTION

Beam current measurements are one of most fundamental measurements for the cyclotron. They are used to measure the transmission at different parts of the beam lines, in particular the transmission at a 4 cm thick graphite target (the so-called target E) for muon and pion production. Transmission measurements at this point are very important. If a portion of the beam were to bypass the target E, the beam footprint on the next target (the SIN-Q spallation neutron source target) could be reduced. This would lead to an overheating of the SIN-Q target surface. Thus, to avoid such possible damage, the transmission at this point must be carefully monitored.

One of the current monitors used for the target E transmission measurement is placed in vacuum behind the graphite target. This monitor, called MHC5, is subject to heavy heat load due to the energy deposition of the scattered particles. The temperature could reach 200°C due to poor heat conduction and low emissivity of the monitor. The resulting mechanical thermal expansion induces a drift of the resonance frequency. The amplification factor of the resonator is then modified leading to a calibration drift. Because of the dynamic nature of this effect, it was not possible to solve this problem by calibrating the monitor at different beam intensities.

Based on these observations, a new current monitor with improved cooling was designed and built. It has an active water cooling system, its surface was blackened to increase the radiation cooling and its mechanical structure was improved for better heat conduction. Temperature sensors were also installed to monitor the cooling efficiency. Simulations and laboratory tests were also performed so that temperature variations would not affect the resonance characteristics of the monitor.

Even with these improved cooling features, the monitor exhibited some anomalous gain drifts up to 30% during operation at high current (>1mA). This problem will be more severe for future high intensity beam operation (3 mA). For this reason, it was necessary to implement a drift compensation that could deal with these dynamic changes.

*pierre-andre.duperrex@psi.ch

RESONATOR AND HEAT LOAD

Measurement Principle

The current monitor consists of a re-entrant resonator , symmetric around proton beam pipe. The open-end gap in the beam pipe couples some of the wall current into the resonator. This gap acts also as a capacitor and determines the resonance frequency. The resonance frequency is set to 101.26 MHz, the 2nd harmonic of the proton beam bunch frequency. This harmonic is used because of the better signal-to-noise ratio, the RF noise components from the generator being mainly at the odd harmonics. No significant shape dependency of the 2nd harmonic amplitude for relatively short beam pulses is expected [1]. The oscillating magnetic field in the resonator is measured using a magnetic pick-up loop, the signal being proportional to the beam current. Advantages of such resonator are that its construction is simple and it is rugged with respect to radiation. Disadvantages are that it is sensitive to temperature and it is not an absolute measurement; the signal has to be calibrated using another current monitor.

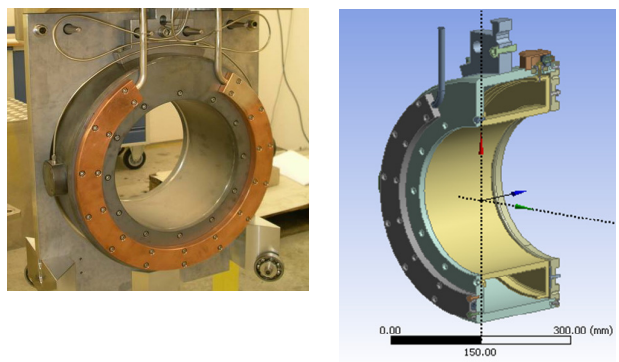

Figure 1: Current monitor ready for installation with the water cooling circuitry at the beam entry side (left). The cavity structure is shown in a half-cut drawing (right).

Mechanical Design

The monitor is made of aluminium (Anticorodal 110), with a 10µm coating layer of silver to improve the electrical conductivity. The inner diameter is 225mm, the outer diameter 420mm, its height 224mm. The capacitor

gap is 4mm wide and small movable plates are used for the fine tuning of the resonance. It has an active water cooling system (maximum water speed: 2m/s).

The monitor itself is in vacuum and the external surfaces were chemically blackened to increase the emissivity for additional cooling. Some tests have been performed to measure the emissivity of various coatings. Without blackening the emissivity is smaller than 5%. The emissivity is between 30% and 60% for either sulphur treated silver or oxidized copper coated aluminium plates. It depends not only on the sort of coating but also on the quality and on the thickness of the coating itself.

Resonance Condition

The resonance condition is derived as followed. The monitor can be considered as a coaxial transmission line with a shorted load.

The characteristic impedance of a coaxial line is:

$$Z_o = \sqrt{\frac{L_{coax}}{C_{coax}}} = \sqrt{\frac{\frac{\mu}{2\pi}\ln(b/a)}{\frac{2\pi\varepsilon}{\ln(b/a)}}} = \frac{1}{2\pi}\sqrt{\mu/\varepsilon}\,\ln(b/a) \cong 60.\ln(b/a)$$

where b is the inner radius of the outer conductor, a is the outer radius of the inner conductor, ε the dielectric constant and μ the magnetic permeability.

The impedance Z_i as seen at the entrance of the resonator will then be given by:

$$Z_i = j\,Z_o \tan\left(\frac{2\pi L}{\lambda_m}\right)$$

where L is the resonator length, Z_o the characteristic impedance of the transmission line, and λ_m the resonant wavelength. For resonator length smaller than $\lambda_m/4$ the impedance is inductive. As for a parallel tuned circuit where the reactance is zero at the resonance:

$$j\,\omega_m\,L_{induct.} = -\frac{1}{j\,\omega_m\,C}$$

the resonance is obtained at the frequency for which the shunt capacitor C_{shunt} compensates Z_i:

$$Z_i = -\frac{1}{j\,\omega_m\,C_{shunt}} = -\frac{\lambda_m}{j\,2\pi\,c\,C_{shunt}}$$

with ω_m the resonance angular frequency and c the speed of light.

The resonance condition can then be expressed as:

$$\tan\left(\frac{2\pi L}{\lambda_m}\right) = \frac{\lambda_m}{2\pi\,c\,C_{shunt}\,Z_o}$$

The previous equation may be rewritten as:

$$\frac{2\pi L}{\lambda_m} = arct\left(\frac{\lambda_m}{2\pi\,c\,C_{shunt}\,Z_o}\right)$$

The right side of the last equation is known as the "universal tuning curve" (see Fig.2).

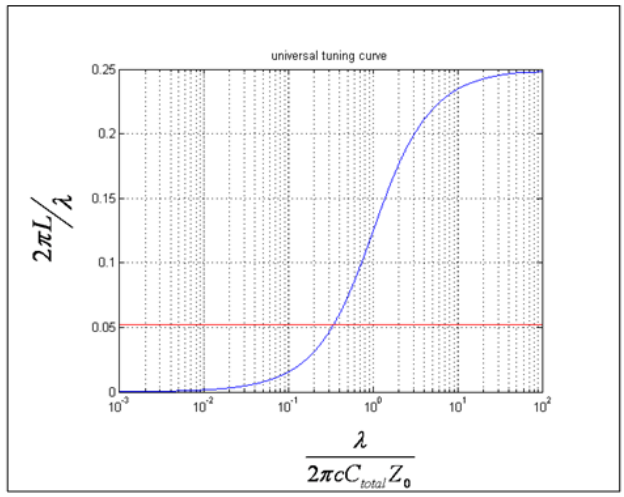

Figure 2: The "universal tuning curve" for re-entrant coaxial resonators establishes the relation between the resonator length (y-axis) and the required C value (x-axis). The red line corresponds to MHC5 conditions.

Heat Load Effects

The predicted heat load on the MHC5 due to the shower particles is about 230W for a 2mA beam [2]. Without water cooling, the monitor would easily reach 200° C.

Bench tests of the water cooling system have been performed before the installation of the monitor on the beam line. External resonant circuits have been added to compensate the temperature drifts. Gain drifts smaller than 0.3dB were measured for the expected temperature variations during beam operation (30 to 70 °C), as shown in Fig.3.

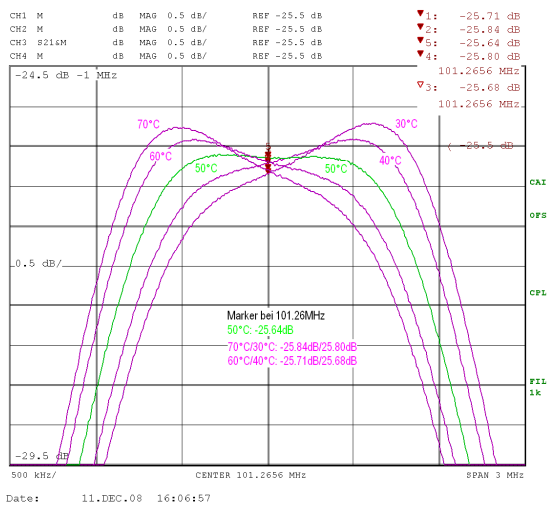

Figure 3: Transfer function of the MHC5 measured at different temperatures. The gain variation at 101.26MHz is smaller than 0.3 dB in laboratory conditions.

However, the observed gain drifts during operation are larger than those measured on the test bench. These larger than expected drifts are induced by the non-uniform temperature distribution, deforming the resonator (see

Fig.4), shifting the resonance frequency and modifying the gain around the resonance frequency [3].

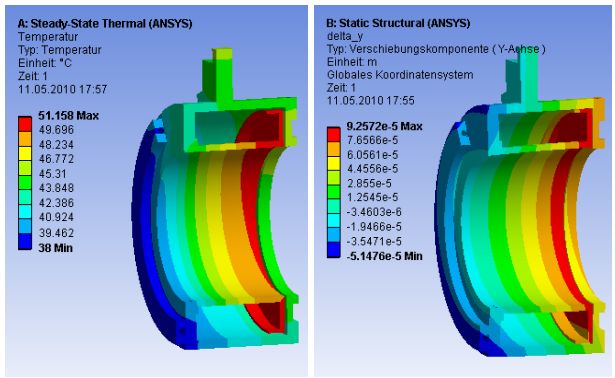

Figure 4: Calculated temperature (left) and horizontal deformation (right) of MHC5 at 1.32 mA.

It was thus necessary to implement a drift compensation method that could account for these dynamic changes during beam operation.

ON-LINE DRIFT COMPENSATION

Compensation Principle

The principle of this new scheme is to use two pilot signals whose frequency is close enough to the RF 2nd harmonic (101.26MHz) to get an estimate of the resonator gain at the RF 2nd harmonic.

The two pilot signals are feed into the resonator and measured using a second magnetic pick-up loop identical to the one used for the current measurement. The comparison of the pilot signal amplitude at the receiver side with the one at the emitter side is a measure of the resonator gain at the pilot frequency. The results obtained at the two different pilot frequencies can then be averaged and give that way an estimate of the resonator gain at the RF frequency.

The frequency difference between the pilot signals and the beam signal has to be large enough to avoid interference with the standard current monitor electronics but small enough so that the average of the two pilot signals can provide a good estimate of the gain.

An earlier drift compensation scheme using a single pilot signal 600 kHz off the resonator frequency was successfully tested to investigate the potential of such a method [2].

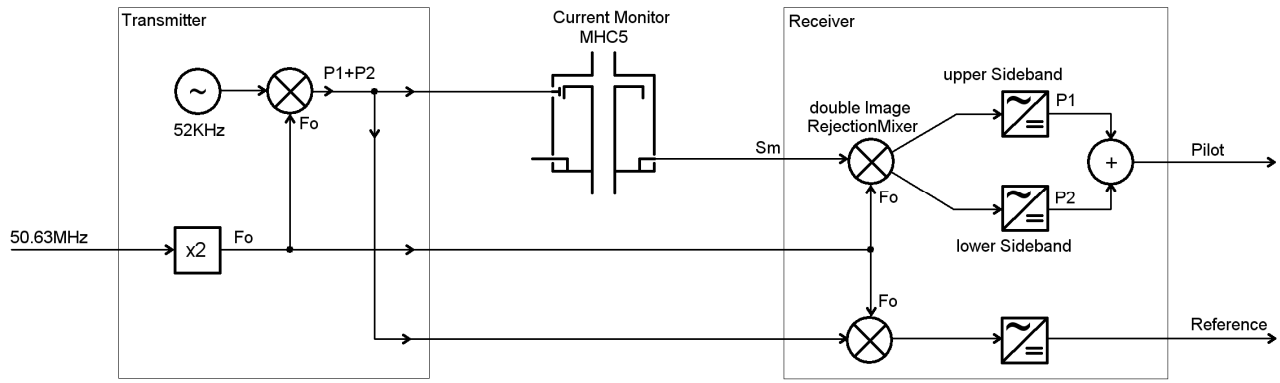

Figure 5: Schematic of signal measurements for the on-line drift compensation. A 52 kHz baseband signal is mixed with the second RF harmonic and feed into the current monitor resonator. The signals are then measured using double image rejection mixers. The ratio Pilot/Reference provides an estimate of the resonator gain.

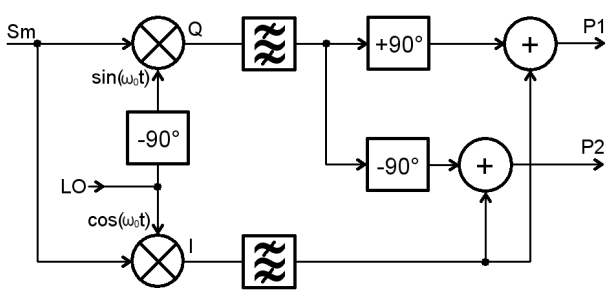

Figure 6: Details of the double image rejection scheme. The Q demodulated component is phase shifted and the resulting signals are recombined with the in-phase signal.

Electronics and Signal Processing

A 52 kHz baseband signal is mixed with the second RF harmonic to generate two pilot signals 52kHz off the 101.26MHz frequency. The resulting signal is feed into the current monitor resonator (Fig.5). These pilot signals are then measured using as sensor a pick-up coil identical to the one used for the current measurements. To separately measure the amplitude of both pilot signals, a double image rejection mixer, shown in Fig.6, has been used. It is a I/Q demodulator followed by a couple of 90 deg. phase shifting before a recombination of the demodulated signals.

The results can be derived analytically as follows. The measured pick-up signal S_m contains the two pilot signals as well as the beam signal:

$$S_m = P_{10}.\cos(\omega_1.t+\phi_1) + P_{20}.\cos(\omega_2.t+\phi_2) + S_{beam}.\cos(\omega_0.t)$$

Where ω_o the angular frequency of the RF 2nd harmonic, $\omega_1=\omega_o-\Delta\omega$ and $\omega_2=\omega_o+\Delta\omega$ the angular frequency of the pilot signals, with $\Delta\omega/2\pi$=52 kHz, P_{10} (resp. P_{20}) the amplitude of the first (resp. second) pilot signal and S_{beam} the amplitude of the beam signal.

After mixing down the signals with the image rejection, a band-pass filter centered at the original pilot frequency eliminates the undesired high frequency components and as well as the beam signal contribution (DC component).

The resulting base-band in-phase (I) and quadrature phase (Q) signals are then:

$$S_I(t) = \frac{1}{2}P_{10}.\cos(\Delta\omega.t-\phi_1) + \frac{1}{2}P_{20}.\cos(\Delta\omega.t+\phi_2)$$

$$S_Q(t) = \frac{1}{2}P_{10}.\sin(\Delta\omega.t-\phi_1) - \frac{1}{2}P_{20}.\sin(\Delta\omega.t+\phi_2)$$

By introducing 90deg. phase shifts on the Q output:

$$S_{Q+90\deg}(t) = \frac{1}{2}P_{10}.\cos(\Delta\omega.t-\phi_1) - \frac{1}{2}P_{20}.\cos(\Delta\omega.t+\phi_2)$$

$$S_{Q-90\deg}(t) = -\frac{1}{2}P_{10}.\cos(\Delta\omega.t-\phi_1) + \frac{1}{2}P_{20}.\cos(\Delta\omega.t+\phi_2)$$

The two pilot signals can then be extracted:

$$S_I(t) + S_{Q+90\deg}(t) = P_{10}.\cos(\Delta\omega.t-\phi_1)$$

$$S_I(t) + S_{Q-90\deg}(t) = P_{20}.\cos(\Delta\omega.t+\phi_2)$$

That way, the pilot signals are separated and their amplitude independently measured. An average is then performed to estimate the level of a pilot signal at 101.26MHz.

After digitization of the averaged pilot and reference signals the Reference/Pilot ratio is then calculated and used as additional scaling factor for the MHC5 current signal:

$$MHC5_{calibrated} = K.\frac{S_{Reference}}{S_{Pilot}}.MHC5_{raw}$$

K being a constant calibration factor that is determined once for all at the beginning of the measurements.

RESULTS

Off-line Analysis

Before implementing the on-line drift compensation scheme in the accelerator control system, some off-line analysis was performed.

In Fig.7, the calibration factor calculated with the pilot drift compensation scheme is compared with the, one that can be deduced using the signal from the MHC6 current monitor located further down the beamline. The MHC6 current monitor is not subject to such heat load and is found to be stable. By assuming that MHC5 and MHC6 are measuring the same current (the beam losses between them are considered to be small enough to be neglected), the MHC5 scale factor can be compared. After 2.5days of operation, the MHC5 cooling system was switched off, the MHC5 temperature rose from 40 to 90°C and the calibration factor changed by 30%..

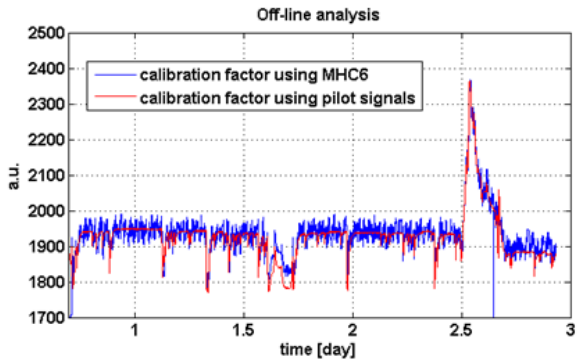

Figure 7: Off-line calibration. Even for a 30% variation, the calibration factor deduced from the pilot signals (red line) matches the one using MHC6, a second current monitor (blue line) further down the beam line.

On-line Results

Figure 8 shows the performance as the new drift compensation scheme was switched on. The MHC5 measurements remain similar to the MHC6 measurements (see the plotted MH5/MHC6 ratio). This shows that the new calibration is working correctly. Changes in the calibration parameter values for the MHC5 can be observed. These are due to cooling effects after a beam loss or smaller beam currents. The comparison between MHC5 and MHC6 measurements confirm that even for these condition changes the current measurement shows improved stability.

The ion source was changed during the 2010 maintenance period and the new one presented wider noise spectra. As a result, the original pilot signals had to be moved from 52kHz to 80kHz off the RF frequency to avoid interference.

Figure 9 presents the performance of the present system with a 80kHz pilot frequency. The excellent agreement between MHC5 and MHC6 indicates that the accuracy is better than 1%, except for beam current smaller than 0.3mA. In this lower beam current range the electronics introduces a 1 to 2% distortion.

CONCLUSION

Heavy heat load on the MHC5 resonant transmission line monitor was a challenge for beam current and transmission measurements. The new drift compensation scheme using two pilot signals close to the resonant frequency of the monitor provides accurate beam current measurements for transient beam load conditions that lead to thermal changes in the resonator gain.

This innovative scheme may have wider applications where resonant systems are subject to uncontrolled drifts.

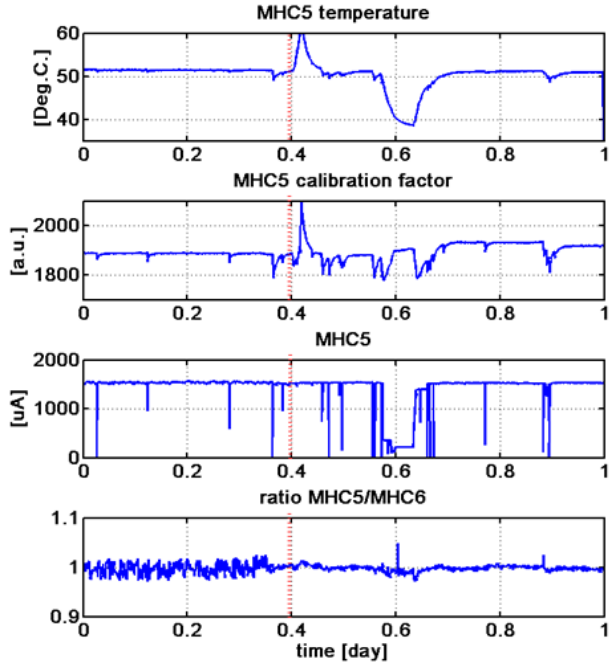

Figure 8: Transient behaviour of the new drift compensation scheme. At t=0.4day the on-line calibration is switched on.

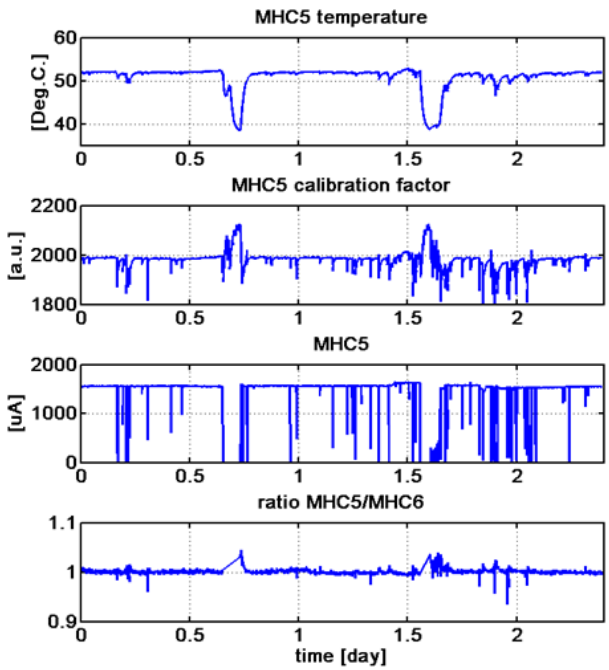

Figure 9: Present performance of the drift compensation system with a 80kHz pilot frequency. The MHC5/MHC6 beam current ratio is indicative of the calibration accuracy that can be achieved by this system.

REFERENCES

[1] R. Reimann, M. Rüede, "Strommonitor für die Messung eines gepulsten Ionenstrahls", Nucl. Instr. Meth. 129 (1975) 53.

[2] P.A. Duperrex, P. Baumann, S. Joray, D. Kiselev, Y. Lee, U. Müller, „Design and operation of a current monitor under heavy heat load" DIPAC'2009, May 2009, TUPD20, p.336 (2009).

[3] Y. Lee "Simulation based Analysis of the anomalous RF drifts of a Current Monitor at the PSI Proton Accelerator Facilities", IPAC2010, May 2010, MOPEC072.